1973

THERMAL RESISTANCE AT SMOOTH-SPHERE/ROUGH-FLAT CONTACTS: THEORETICAL ANALYSIS

S.S. Burde* and M.M. Yovanovich+
University of Waterloo, Waterloo, Ontario, Canada

Abstract

Steady-state thermal constriction resistance between smooth spheres and rough flats in contact is analyzed by means of a mechanical model that considers the elastic and plastic deformation of the mean planes and roughness, respectively. It incorporates a variable contact size and distribution. The thermal model predicts the resistance of contact areas when the microcontacts are circular or elliptical under isothermal or uniform flux conditions. Plots of a novel dimensionless contact resistance vs the dimensionless surface roughness for several values of the dimensionless asperity slope are obtained for some selected dimensionless hardness values.

Nomenclature

A_1 = area of the flat
A_c = contact area
A_H = Hertzian area
A_r = real contact area
a = microcontact radius
B = complete elliptic integral
b = cell half-width
D = sphere diameter
$d_{ij} = \alpha_i / [(\rho_j \cos\theta_j + \mu_k - \rho_i \cos\theta_i)^2 + (\rho_j \sin\theta_j + \nu_k - \rho_i \sin\theta_i)^2]^{1/2}$
E_1, E_2 = Young's elastic modulus of contacting solids 1 and 2
$f_{ij} = \sin^{-1} d_{ij}$, Eqs. (7) and (9)

Presented as Paper 78-871 at the 2nd AIAA/ASME Thermophysics and Heat Transfer Conference, Palo Alto, Calif., May 24-26, 1978.

*Post Doctoral Fellow, Thermal Engineering Group, Department of Mechanical Engineering.

+Professor, Thermal Engineering Group, Department of Mechanical Engineering.

f_{ij} = $d_{ij}B(d_{ij})$, Eqs. (8) and (10)
f_{12} = radiant interchange factor
G = summation term $\sum_{i=1}^{M} \alpha_i^2$
H = microhardness
H^* = dimensionless hardness, $\pi H\,[(9/64)(D^2\Delta^2/N)]^{1/3}$
M = number of microcontacts
$\dot{m}$ = absolute average asperity slope
$\dot{m}^*$ = dimensionless asperity slope $\dot{m}/H\Delta$
N = contact load
n = number of summation term
$\bar{n}$ = number of microcontacts per unit area
p_c = contact pressure
Q = heat flow rate
R_c = constriction resistance
R_r = radiative resistance
R_t = contact resistance
r = radial coordinate
r_{cont} = contour radius
r_e = contact radius
r_H = Hertzian radius $[(3/8)ND\Delta]^{1/3}$
S_1 = $1/(1 + 2.5/\dot{m}^{*1.2})$
S_2 = $1/(1 + 1.05/\dot{m}^*)$
T = temperature
T_m = mean surface temperature
W = summation term $\sum_{i=1}^{M} \dfrac{\alpha_i^2}{\sqrt{1 - (\rho_i/\rho_e)^2}}$
w = weight factor
Y = separation between the mean surfaces at some r
α = dimensionless microcontact radius a/r_H
Δ = physical parameter $(1 - \nu_1^2)/E_1 + (1 - \nu_2^2)/E_2$
ζ = dimensionless cell half-width b/r_H
η = dimensionless separation $Y/\sigma\sqrt{2}$
λ_1, λ_2 = thermal conductivity of contacting solids 1 and 2
λ_s = harmonic mean thermal conductivity $2\lambda_1\lambda_2/(\lambda_1 + \lambda_2)$
μ = dimensionless coordinate x/r_H
ν = dimensionless coordinate y/r_H
ν_1, ν_2 = Poisson's ratio of contacting solids 1 and 2
ρ = dimensionless radius r/r_H
ρ_{cont} = dimensionless contour radius r_{cont}/r_H
σ = root-mean-square (rms) roughness
$\bar{\sigma}$ = Stefan-Boltzman constant
σ^* = dimensionless roughness $\pi\sigma[(3/8)(D/N^2\Delta^2)]^{1/3}$

Introduction

There are large number of papers in the literature concerning surface topography, deformation analysis, and the contact resistance between two rough, flat or wavy solids. This problem is of significant importance, for example, in aerospace and nuclear industries. The authors[1-9] assumed in their contact models that all microcontacts are of equal radius and that they are distributed uniformly in the contour area formed between rough, wavy surfaces in contact or in the apparent area in case of rough, flat surfaces in contact. Thermal models are available[4-7,10-14] for predicting the constriction resistance of a microcontact on a half-space or on a right circular cylinder under some thermal boundary condition. By the principle of superposition of microresistances and macroresistance, the total constriction resistance is equal to the sum of the microresistances and the macroresistance.

The assumptions that the microcontacts are of equal radius and distributed uniformly in the apparent area between the rough, flat surfaces in contact are good approximations for a certain range of contact pressure. However, these assumptions are questionable in case of the rough, wavy surfaces in contact where the pressure at the load axis is maximum and decreases along the radial coordinate. As a result of this pressure distribution, the microcontacts would be denser near the load axis and of larger radius than those away from the axis. It is almost impossible to determine the heat flux

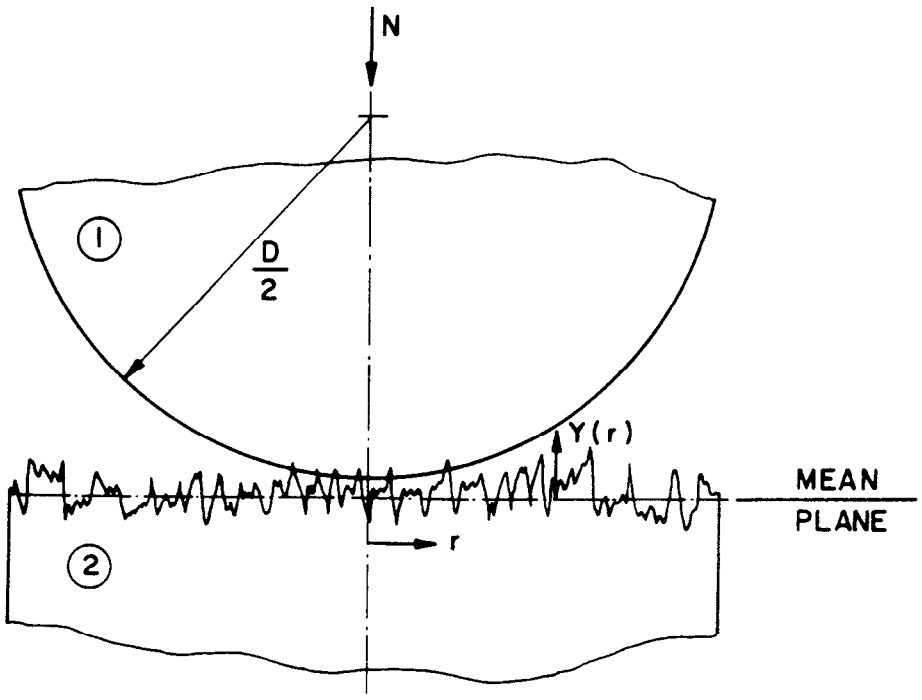

Fig. 1 Model of smooth-sphere/rough-flat surface contact.

tube radius associated with the microcontacts within acceptable accuracy when the microcontact distribution is nonuniform. Consequently, the existing models of predicting the microresistance fail to give the result, and therefore the method of superposition of resistances cannot be applied in determining the constriction resistance.

The objective of the present investigation is to derive the expressions on a statistical basis wherever required to determine the microcontact size distribution and the extent of the contact area for a model of smooth-sphere/rough-flat contact under load, and to develop a more general method of determining the constriction resistance based on either uniform flux or isothermal boundary condition on the microcontacts and the contact area. The interstitial fluid is assumed to be absent in the present work. The radiation resistance will be studied based upon the decoupled model and will be added in parallel to the constriction resistance.

Mechanical Analysis

Contact Model

Consider a contact model in which a smooth sphere 1 of diameter D is in contact with a rough, softer flat 2 (Fig. 1).

It is assumed for the mechanical analysis of the contact problem that 1) the roughness heights from the mean plane have a gaussian distribution; 2) the asperities deform plastically, whereas the sublayers and the bulk of the solids undergo elastic deformation; 3) the plastic deformation of the contacting asperities is related to the hardness of the softer solid; 4) the problem will be analyzed for first contact where the plastic deformation of asperities is the dominant mode of the mechanical interaction; 5) the contacting surfaces are clean and isotropic and remain so during the contact; 6) the contacting solids are thick relative to the roughness heights; 7) the contact occurs under static loading, i.e., vibrational effects are absent; and 8) the tangential forces due to friction have negligible effect upon the compressive load.

Separation

When a hard, smooth sphere and a softer, rough flat first are brought into contact, they touch only at a few points. These points and the mean surfaces of both solids undergo deformation by the application of the load. Consequently, the separation between the mean surfaces decreases, thereby increasing the number of discrete contact spots, as well as the deformed area over the asperities. The separation is minimum

at the load axis and increases continuously in a certain fashion along the radial coordinate r. The separation Y(r) for small r can be obtained by means of Hankel transforms (Terezawa's solution)[15].

Real Contact Area

The real contact area between the surfaces is the sum of the areas of the individual contact spots. The real contact area at any asperity tip is usually very small compared to the contour area, and they may differ from one another depending upon their location relative to the load axis. The pressure distribution on the contact plane is assumed to be symmetrical about the load axis, with maximum pressure on the load axis and zero far away from it. Assuming this, the contact area near the axis will be stressed more than that away from it; therefore, the contact spots near the axis will be larger than those away from the axis. The stress on the deformed asperities is assumed to be the microhardness H of the material determined in a Vickers test, and that work-hardening is negligible.

Pressure Distribution

The force balance on the elemental real area and the elemental contact area is considered and the following relationship is obtained for the local pressure as a function of the local separation $\eta(\rho)$ between the mean planes:

$$p_c(\rho) = (HS_1/2)\ \mathrm{erfc}\ [\eta(\rho)] \tag{1}$$

Mikic[16] showed that the elastic deformation under the contact points is significant under light contact loads if the modulus of elasticity of the surface is not very large. The parameter S_1 takes this effect into account.

The external load N applied on the contact must be distributed over the contact spots. The spots located near the origin will share a larger load than those farther away because of the equivalent pressure distribution. Also, the load must be equal to the integrated value of the pressure over the contact area, i.e.,

$$N = \iint_{A_c} p_c(\rho)\ dA_c \tag{2}$$

Equation for the separation and Eqs. (1) and (2) are required for determining the pressure and the corresponding separation between the mean surfaces along the radius ρ. These equations

are nondimensionalized and are functions of the dimensionless parameters H^*, σ^*, and $\dot{m}^*$ alone. Their values are required for the numerical solution by means of the iterative procedure described in Ref. 15. The pressure distribution was obtained for certain selected values of H^*, σ^*, and $\dot{m}^*$ corresponding to a practical range of geometric and surface characteristics. It is evident that there are many combinations of the geometric and surface characteristics, physical properties, and mechanical load giving the same values of the parameters H^*, σ^*, and $\dot{m}^*$ and therefore the same pressure distribution.

Number of Microcontacts

The expression for the contact spot density $\bar{n}(\rho)$ at the separation $\eta(\rho)$ is[8]

$$\bar{n}(\rho) = \left[\frac{\dot{m}^* H^*}{4 r_H \sigma^*}\right]^2 \frac{\exp[-2\eta^2(\rho)]}{\operatorname{erfc}[\eta(\rho)]} \tag{3}$$

The total number of contact spots can be obtained by integrating Eq. (3) numerically over the contact area. It should be noted that the number of contact spots is directly proportional to the square of the average roughness slope. Surfaces prepared by different particles under different conditions will have different average slopes, although the roughness may be the same, resulting in large differences in the number of microcontacts [17].

Microcontact Distribution

As a result of the contact pressure falling continuously along the radius, it is expected that microcontacts will be farther apart from those nearer to the origin. In order to describe this effect, a model of microcontact distribution is considered [17] where there are a certain number of microcontacts in various rows of annular areas along the radius, the number being different in each row. The area associated with a microcontact, called a cell, is considered on a line similar to a heat flux tube associated with a microcontact when microcontacts are distributed uniformly. The cell area is approximated by a square of side 2b. The expression for the dimensionless cell size $\zeta(\rho)$ as a function of the separation $\eta(\rho)$ is [17]

$$\zeta(\rho) = (2\sigma^*/\dot{m}^* H^*) \exp[\eta^2(\rho)] \sqrt{\operatorname{erfc}[\eta(\rho)]} \tag{4}$$

For given contact parameters, Eq. (4) shows that the cell half-width is a minimum on the load axis and increases along the

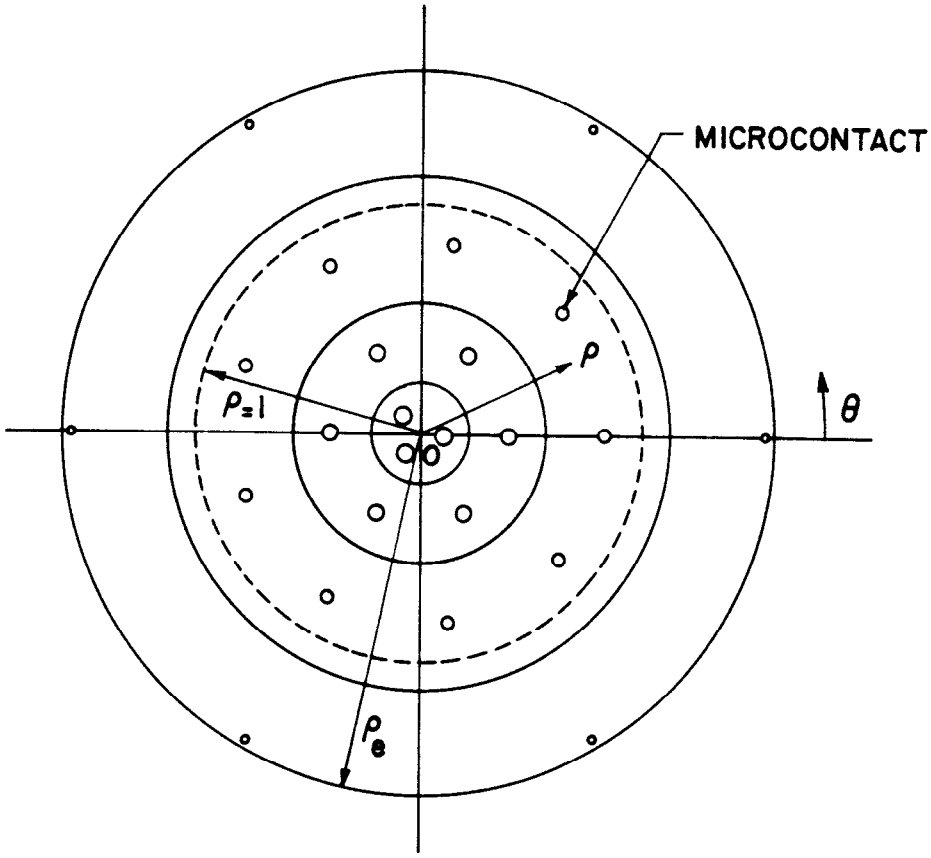

Fig. 2 Model of microcontact distribution in the contact area.

radius. A model of the first row of an annular area is considered, and the method of determining subsequent rows of annular areas is described in Ref. 17. The procedure of determining the number of microcontacts M_i associated with the ith annular region is given in Ref. 17. These microcontacts are distributed uniformly on the line corresponding to the mean radius of the annular region. The microcontact radius in an annular area will be discussed next.

Microcontact Radius

It is assumed in the present analysis that all microcontacts are circular and that the microcontact size varies as a function of the radius alone. The following expression is developed for the microcontact radius $\alpha(\rho)$ as a function of the separation and other contact parameters [17]:

$$\alpha(\rho) = \frac{4S_1\sigma^*}{\sqrt{2\pi}\, S_2 m^* H^*} \exp[\eta^2(\rho)]\ \text{erfc}\ [\eta(\rho)] \qquad (5)$$

where S_2 takes into account the effect of the elastic deformation under the contact points [16]. It can be seen from Eq.(5) that the microcontact radius decreases with an increase in the absolute average asperity slope in some manner. This is apparent from the fact that, for a given surface roughness, material properties, and the load, a surface with a large num-

ber of asperities (high absolute average asperity slope) would have greater number of microcontacts and smaller microcontact radius than those for a surface with a few asperities (low absolute average asperity slope). Inspection of Eq.(5) reveals that the microcontact size is maximum at the load axis and decreases along the radius. Equation(5)can be evaluated for the line corresponding to the mean radius ρ_i of the ith annular area to determine the microcontact radius α_i for the probable number of microcontacts M_i. This is repeated for all rows of the annular areas to determine the microcontact radii on the contact area.

Figure 2 shows a model of the contact area of radius ρ_e formed between the contacting solids under a certain load. There are M microcontacts of different radii distributed at known radial coordinates in the annular areas. Physically there is no contact between the solids beyond this radius, and it is quite different from the contour radius defined by the authors [5-7,15]. It is assumed equal to the radius of a circle touching the microcontacts in the last row of annular area (Fig. 2)[17]. The area enclosed by the dotted circle (ρ=1) represents the Hertzian area between contacting smooth solids.

Examination of Eqs. (3-5) indicates that the dimensionless parameters H^*, σ^*, and $\dot{m}^*$ must be maintained constant in order to obtain the same microcontact radii distribution, the number and the microcontact distribution at the interface formed between the contacting solids having various combinations of the surface characteristics, material properties, and load.

If the roughness heights y_1 and y_2 from the mean planes and $|y_1'|$ and $|y_2'|$ of the two rough spherical surfaces have gaussian distribution and are brought into contact under the load, the equations developed here can be applied for predicting the probable microcontact size, the number, and the distribution in the contact area. In this case y is replaced by y_1+y_2. The standard deviation for the height distribution σ and the absolute average asperity slope $\dot{m}$ are replaced by the square-root of the sum of the squares of the respective values for the two surfaces. If the slopes $|y_1'|$ and $|y_2'|$ are approximately constant or have different values, $\dot{m}$ is replaced by the larger of two slopes $\dot{m}_1$ and $\dot{m}_2$.[5]

Comparison between Present and Existing Models

The present contact model is somewhat similar to that of Yip [7] because both models assumed the contacting rough surf-

aces to have a gaussian height distribution and that the mean surfaces and the asperities undergo elastic and plastic deformation, respectively. The important differences in these models can be found in the determination of the separation between the mean planes and the resulting microcontact size and distribution on the contact area. The present model assumes a continuously increasing separation between the mean surfaces as a function of the radius, whereas the Yip model, inappropriately, considered two separation regimes: one consisting of uniform separation within the Hertzian area, and another of increasing separation beyond the Hertzian area.

A typical contact between a smooth sphere and a rough flat under various loads will be considered. The number of microcontacts M, the average microcontact radius $\bar{\alpha}$, and the contact area radius ρ_e are determined for the following contact parameters: D = 28.58 mm, σ = 1.305 μ, m = 0.073, H = 3.923 x 10^9 N/m^2, and Δ = 0.88 x 10^{-11} m^2/N. The results are compared with those given by Yip [7] and are presented in Table 1.

It can be seen from Table 1 that the present model predicts larger contact radii than the contour radii given by Yip's model and Mikic[5] at light contact loads. However, at high contact loads, the contact and the contour radii predicted by all the models are close to one another. It is also observed that the present model predicts more microcontacts and consequently smaller average microcontact radii than those given by Yip's model at light loads. The present model predicts a certain microcontact radius distribution along the contact radius. Microcontacts near the load axis are larger than those near the contact boundary by an order of magnitude, depending upon the load. At loads beyond 360 N the present model predicts fewer microcontacts, and consequently larger

Table 1 Comparison between present and Yip's model[12]

Contact load, N	ρ_e ρ_{cont}		M		$\bar{\alpha}$	
	Present model	Yip	Present model	Yip	Present model	Yip
26.1	2.224	1.433	28	16	.0644	.0852
75.1	1.712	1.284	56	35	.0543	.0687
146.3	1.500	1.224	80	57	.0508	.0602
360.0	1.307	1.155	120	104	.0482	.0518
690.4	1.200	1.112	146	152	.0487	.0477

average microcontact radius, than those given by Yip's model. The difference in the microcontact size along the radius becomes relatively small.

To recapitulate, the proposed mechanical analysis predicts the probable number and radii of microcontacts, their distribution, and the contact area radius for the contact model. It appears to be more appropriate than the analyses available in the literature from the physical standpoint. Its importance will be clear when we discuss the thermal analysis to determine the constriction resistance.

Thermal Analysis

It is important to note that the metal-to-metal conduction is the dominant mode of heat transfer across the interface formed between the contacting solids. Other modes of heat transfer, such as the conduction and the convection through the interstitial fluid, are absent when the contact occurs in a vacuum environment. Radiation heat transfer across the gaps is usually quite small; however, it has been taken into account by considering an approximate model of radiative resistance.

A mathematical model of the constriction resistance will be discussed based on a known microcontact distribution on the contact area and some thermal boundary condition on the microcontacts and the contact area. For practical purposes, the contact area will be assumed to be under either of the two well-known boundary conditions: 1) uniform temperature, or 2) uniform heat flux. Similarly, the microcontacts may be assumed under either boundary condition.

It is assumed further in the thermal analysis that 1) the contacting surfaces are free from oxides, 2) the contact occurs in a vacuum environment, 3) the microcontacts are on a plane, 4) heat flow rate is steady, and 5) the noncontact region in the contact area is perfectly insulated. Expressions will be developed in the following sections for the contact constriction resistance under four possible combinations of the thermal boundary conditions on the microcontacts and the contact area.

Constriction Resistance Definition

The thermal constriction resistance R_c of the contact area (Fig. 2) is defined as the average temperature of the real contact area A_r divided by the total heat flow rate Q, i.e.,

radius ρ_e on a half-space where the microcontacts are assumed to be under uniform heat flux condition. The dimensionless resistance of the contact area between two solids under these conditions can be determined by the following equation [17]:

$$\lambda_s \sqrt{A_H}\, R^q_{cT} = \frac{4}{\pi^{3/2} G_W} \sum_{i=1}^{M} \frac{\alpha_i}{\sqrt{1 - (\rho_i/\rho_e)^2}} \left[\frac{4}{3} \alpha_i^2 + \sum_{j \neq i}^{M} \alpha_j^2 \sum_{k=1}^{n} w_k f_{ij}(\mu_k, \nu_k) \right] \tag{8}$$

Constriction Resistance: Contact Area under Uniform Heat Flux

Isothermal Microcontacts. The dimensionless constriction resistance of the contact area under uniform heat flux and the microcontacts under isothermal condition can be obtained by means of the following expression [17]:

$$\lambda_s \sqrt{A_H}\, R^T_{cq} = \frac{1}{\sqrt{\pi} G^2} \sum_{i=1}^{M} \alpha_i \left[\frac{\pi}{2} \alpha_i^2 + \sum_{j \neq i}^{M} \alpha_j^2 \sum_{k=1}^{n} w_k f_{ij}(\mu_k, \nu_k) \right] \tag{9}$$

where the subscript q refers to the uniform flux on the contact area, and the superscript T refers to the isothermal boundary condition on the microcontacts.

Microcontacts under Uniform Heat Flux. The dimensionless constriction resistance of the contact area can be determined by the following expression, where the microcontacts are assumed to be under the same uniform flux [17]:

$$\lambda_s \sqrt{A_H}\, R^q_{cq} = \frac{4}{\pi^{3/2} G^2} \sum_{i=1}^{M} \alpha_i \left[\frac{4}{3} \alpha_i^2 + \sum_{j \neq i}^{M} \alpha_j^2 \sum_{k=1}^{n} w_k f_{ij}(\mu_k, \nu_k) \right] \tag{10}$$

If the contact area is on a coaxial right circular cylinder, the resistance given by Eqs. (7-10) must be modified to take into account the effect of the cylinder wall on the contact temperature and the resulting drop in the resistance. This situation may occur where a very wavy smooth surface at one end of the cylinder is in contact with a rough flat end of another cylinder at high load. The total constriction resistance in this case is defined as the average temperature of the real contact area minus the average temperature of the cylinder area divided by the heat flow rate across the interface. Expressions for the total resistance have been obtained for the contact area and the microcontacts under the above boundary conditions and are given in Ref. 17.

From the analysis presented here, it is evident that, for a given harmonic mean thermal conductivity of the contacting

solids and the thermal boundary conditions, the constriction resistance merely depends upon the microcontact radii, their number, and their distribution in the contact area. It has been shown in the "Mechanical Analysis" that several combinations of the contacting solids can have the same contact configuration provided that the dimensionless parameters H^*, σ^*, and m^* are maintained constant. It is apparent that these contacting solids would have the same dimensionless resistance.

Radiative Resistance

The contacting surfaces are assumed to be isothermal and are enclosed by a reradiating (insulated) surface. If the surface temperatures are close to each other, the radiative resistance can be determined by the following approximate expression [17]:

$$R_r = 1/4\bar{\sigma}A_1 f_{12} T_m^3 \tag{11}$$

The radiant interchange factor f_{12} can be determined by the method described in Ref. 17.

Contact Resistance

It is assumed in the present thermal analysis that both the constriction and the radiative resistances are independent of each other and that they are connected thermally in parallel. The total resistance of the contact area, R_t, under a vacuum condition is given by the following relation:

$$1/R_t = (1/R_c) + (1/R_r) \tag{12}$$

Comparison between Resistances by the Models

Contact geometries described in Table 1 with known microcontact number and radii distribution in the contact area were considered. The constriction resistances were obtained by means of Eq. (7) for the contact area and the microcontacts under isothermal conditions. The results were obtained for the same boundary conditions by Yip's method (superposition of microscopic and macroscopic resistances). Experiments have been performed by the authors [17] to measure the resistances for several combinations of surface characteristics, material properties, and load including the typical contact. The radiative resistances were determined by Eq. (11) for the measured surface temperatures, and the theoretical contact resistances were obtained by Eq. (12). The radiative resistances were found to be about 20 times the constriction resistances at light loads and about 50 times at high loads. The results are presented in Table 2. It can be seen that the resistances obtained by

Table 2 Comparison between the resistances by present and Yip's model[12]

Contact load, N	Contact resistance, °C/w		
	Measurement	Present model	Yip
26.1	72.81	80.45	101.0
75.1	53.93	57.10	61.63
146.3	46.63	47.44	46.87
360.0	35.20	35.52	33.89
690.4	29.54	29.66	27.09

the present model are closer to the measured values at light loads and also lower than those given by Yip's model. We believe that this is primarily due to more microcontacts distributed in the larger contact area predicted by the proposed mechanical analysis than those given by Yip's model. Thermal analysis also determines the interaction of microcontacts with greater accuracy. At loads higher than 75 N, the agreement between the results by measurement and the proposed model is excellent, while Yip's model predicts resistances lower than the measured values.

Numerical Results

For a given H^*, several contact configurations were obtained by varying the parameters σ^* and $\dot{m}^*$ within the range of industrial applications. The microcontacts and the contact area are assumed isothermal, and the contact area is assumed to be on a half-space. The dimensionless constriction resistances were obtained by means of Eq.(7) for each set of σ^* and $\dot{m}^*$. The results are presented in Figs. 3 - 6 for $H^* = 5$, 10, 25, and 50, respectively. It is noteworthy that the constriction resistance parameters are presented in a compact form to obtain the resistance readily once the parameters H^*, σ^*, and $\dot{m}^*$ are available.

It is noted from the figures that, for a given H^* and σ^*, the resistance increases with decrease in $\dot{m}^*$. In other words, the resistance increases with a decrease in the asperity slope for a given rms roughness, curvature, material properties, and load. This is apparent because a smaller asperity slope yields fewer microcontacts and, as a result, a higher resistance. It is important to realize that, for fixed values of H^* and σ^*, the constriction resistance may be below, equal to, or greater than the resistance of contacting smooth solids under the same conditions, depending upon the asperity slope. It can be

inferred from the results that there are some combinations of the parameters H^* and $\dot{m}^*$ where σ^* has no effect on the resistance whatsoever. For instance, when $H^* = 10$ and $1/\dot{m}^* \approx 0.25$ (Fig. 4), the dimensionless resistance is always 0.886, independent of σ^*. However, the roughness effect is negligible for any asperity slope, as can be seen from the convergence of the $1/\dot{m}^*$ curves at small values of σ^*. This is valid at sufficiently high mechanical loads and can be determined from Figs. 3 - 6 for the given contacting solids.

The preceding discussion confirms the consistency of the results presented in Figs. 3 - 6. Based upon the theoretical and the experimental [17] results, it is expected that the results in Fig. 3 may be about 10% above the actual resistance for σ^* and $1/\dot{m}^*$ greater than 1.0 and 0.4, respectively. For large values of H^*, the results in Figs. 4 - 6 may be about 12% above the actual resistance for σ^* and $1/\dot{m}^*$ greater than 4.0 and 0.4, respectively.

Discussion and Conclusion

A "Mechanical Analysis" is presented for determining the microcontact radius distribution, the number, and the distribution in the contact area formed between a smooth sphere and a rough flat. The roughness heights on the flat solid had

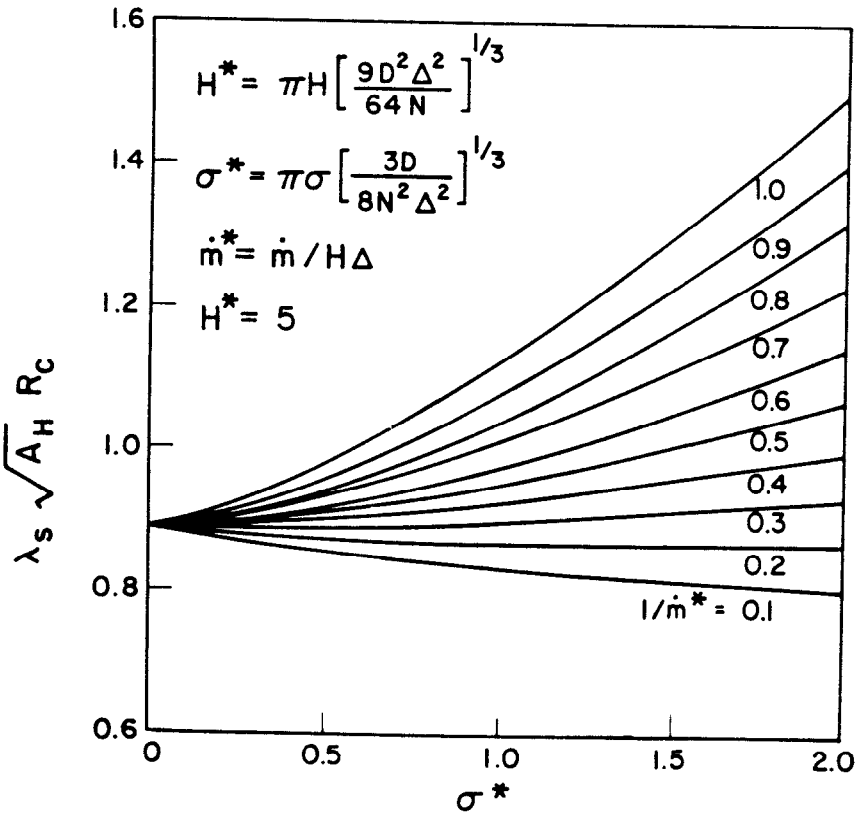

Fig. 3 Dimensionless constriction resistance between rough spheres in contact ($H^* = 5$).

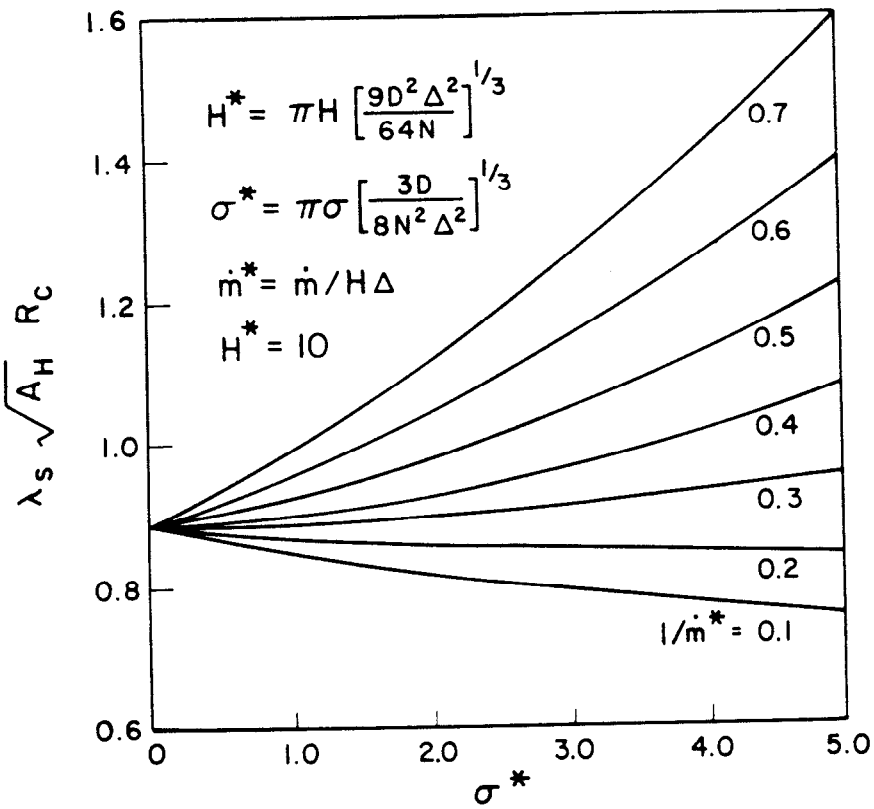

Fig. 4 Dimensionless constriction resistance between rough spheres in contact ($H^* = 10$).

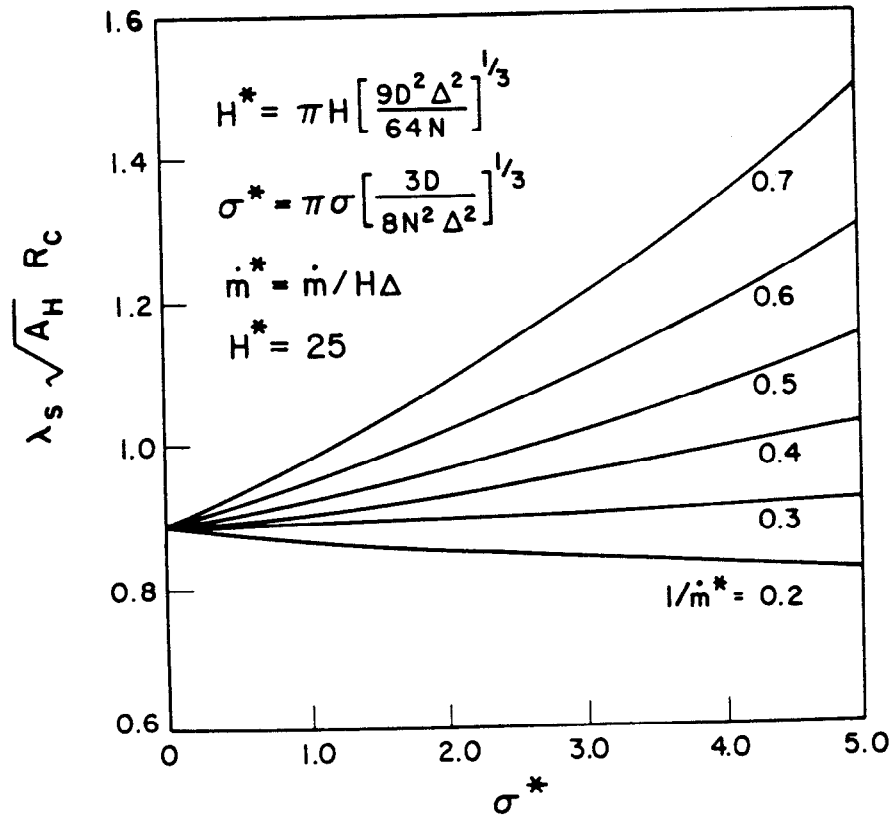

Fig. 5 Dimensionless constriction resistance between rough spheres in contact ($H^* = 25$).

gaussian distribution from the mean plane. A "Thermal Analysis" is considered, and the expressions are developed for determining the contact constriction resistance under various thermal boundary conditions on the microcontacts and the contact area.

The microcontact radius, the number, and the distribution in the contact area obtained by the proposed mechanical model definitely are appropriate to the real contact situation where the separation between the mean surfaces increases, and consequently the contact pressure decreases along the radial coordinate. The thermal analysis presented here is superior to the principle of superposition of microscopic and macroscopic resistances. The proposed model, unlike the superposition method, can be employed in predicting the resistance of a contact area where the microcontacts of different radii are distributed in a known manner. (Coordinates of the microcontacts are known.) Its usefulness in a variety of contact problems is remarkable, especially when it is difficult or impossible to establish the boundary of noncircular contact areas. The superposition method is unable to predict the resistance of such contact areas. The proposed model does not require the artificial and disputable boundary of the contact area when the microcontacts are assumed to be under equal uniform heat flux [17]. This method yields the upper limit of the contact constriction resistance.

The results of the present method are made available in graphical form to allow prediction of constriction resistances between rough spheres in contact, having different combinations of geometry, surface characteristics, material properties, and mechanical load all grouped in the dimensionless parameters H^*, σ^*, and $\dot{m}^*$. It is observed that the roughness effect on the contact resistance is negligible, and, as a result, the contact area acts as a single circular isothermal spot at loads greater than or equal to some load, depending upon the surface characteristics and the material properties. The limiting value of the load can be determined for the selected values of H^* by means of Figs. 3 - 6 with the desired accuracy. The constriction resistance at this load simply becomes $1/2\lambda_s r_H$ and indicates that neither the present theory nor the other theories in the literature are required in predicting the constriction resistance of the contact under high load. The negligible effect of the roughness on the resistance is expected to be valid for other shapes of the contacting smooth solids with the rough flats. The shape of the contact area depends upon the shape of the smooth solid. For instance, a smooth spheroid in contact with a rough flat would result in an elliptical contact area. The microcontacts are

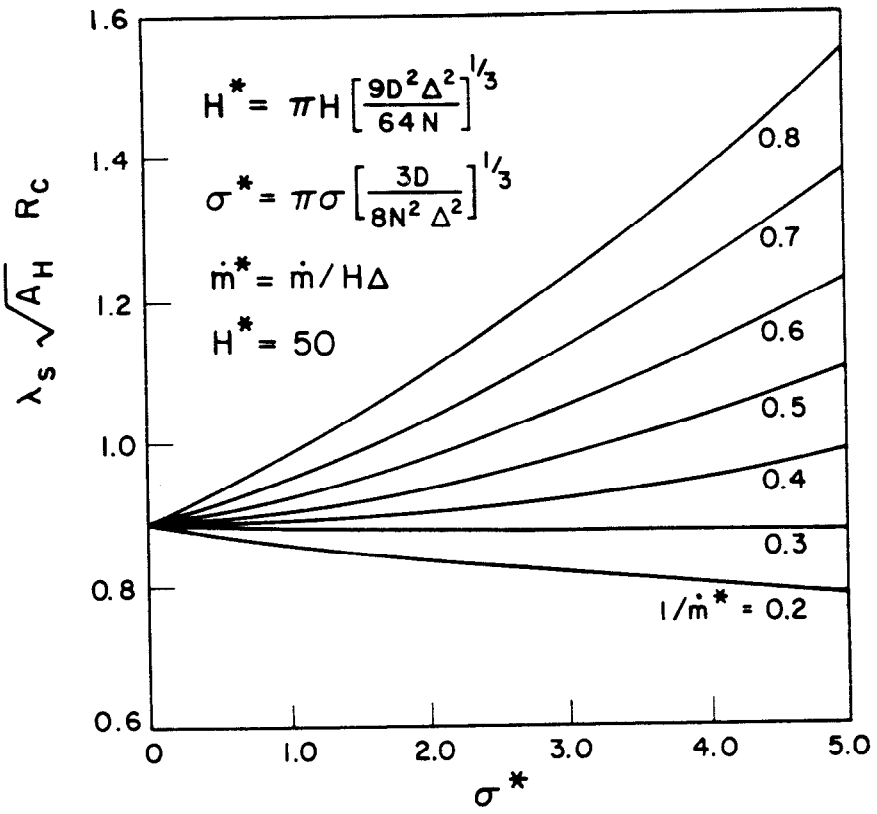

Fig. 6 Dimensionless constriction resistance between rough spheres in contact ($H^* = 50$).

expected to lie on several ellipses within it. The present and other existing models are unable to predict the precise contact area and, consequently, its constriction resistance at any load. At sufficiently high load, it would act like a single elliptical contact spot of the same area and can be computed easily by the elasticity theory for smooth solids in contact. It has been shown that the dimensionless resistance of a single circular contact spot based upon the square root of the area under uniform heat flux varies insignificantly with some change in its size and the shape [19]. In particular, the Hertzian area, unlike the contact area, is unique under all loads and coincides with the contact area under high loads. Therefore, the nondimensionalization of the constriction resistance based upon the square root of the Hertzian area is appropriate. The dimensionless resistance of the single isothermal circular contact spot then becomes 0.886. The dimensionless constriction resistance of the smooth-spheroid/rough-flat contact based upon the square root of its area is approximately 0.886, provided that the shape does not vary too much from the circle [19].

Acknowledgment

The authors thank the National Research Council for its financial support. The authors also acknowledge the fruitful dis-

cussions with G.E. Schneider and J.C. Thompson of the University of Waterloo, and B.B. Mikic of the Massachusetts Institute of Technology.

References

[1] D'Yachenko, P.E., Tolkocheva, N.N., Andreev, G.A., and Karpova, T.M., "The Actual Contact Area Between Touching Surfaces," Consultants Bureau, New York, 1964.

[2] Greenwood, J.A. and Tripp, J.H., "Elastic Contact of Rough Spheres," Burndy Research Div., Rept. 21, Feb. 25, 1965.

[3] Greenwood, J.A. and Williamson, J.B.P., "Contact of Nominally Flat Surfaces," Proceedings of the Royal Society (London), Ser. A, Vol. 295, Dec. 1966, pp. 300-319.

[4] Yovanovich, M.M. and Fenech, H., "Thermal Contact Conductance of Nominally Flat, Rough Surfaces in a Vacuum Environment," AIAA Paper 66-42; also published in Progress in Astronautics and Aeronautics: Thermophysics and Temperature Control, Vol. 18, ed. by G.B. Heller, AIAA, N.Y., 1966, pp. 773-796.

[5] Mikic, B.B., "Thermal Contact Resistance," Massachusetts Inst. of Technology, Sc.D. Thesis, Sept. 1966.

[6] Yovanovich, M.M., "Influence of Surface Roughness and Waviness Upon Thermal Contact Resistance," Massachusetts Inst. of Technology, Sc.D. Thesis, June 1967.

[7] Yip, F.K.C., "Thermal Contact - Constriction Resistance," Univ. of Calgary, Ph.D. Thesis, June 1969.

[8] Mikic, B.B., "Analytical Studies of Contact of Nominally Flat Surfaces; Effect of Previous Loading," Journal of Lubrication Technology, Vol. 93, Oct. 1971, pp. 451-456.

[9] Yovanovich, M.M., "Thermal Contact Resistance: Theory and Application," Mechanical Engineering Dept., Univ. of Waterloo, ME 758 Notes, 1971.

[10] Cetinkale, T.N. and Fishenden, M., "Thermal Conductance of Metal Surfaces in Contact," Conference of the Institute of Mechanical Engineers and ASME, Sept. 1951, pp. 271-275.

[11] Holm, R., Electric Contacts Handbook, Springer-Verlag, Berlin, 1958.

[12]Fenech, H. and Rohsenow, W.M., "Thermal Conductance of Metallic Surfaces in Contact," Atomic Energy Commission, Rept. NYO-2136, May 1959.

[13]Roess, L.C., "Theory of Spreading Conductance," Beacon Laboratories of Texas Co., Beacon, N.Y., unpublished rept., appendix A.

[14]Clausing, A.M. and Chao, B.T., "Thermal Contact Resistance in a Vacuum Environment," NASA, Univ. of Illinois, ME-TN-242-1, Aug. 1963.

[15]Roca, R.T., "Thermal Contact Resistance in a Non-Ideal Joint," Massachusetts Inst. of Technology, Sc.D. Thesis, Nov. 1971.

[16]Mikic, B.B., "Thermal Contact Conductance; Theoretical Considerations," International Journal of Heat and Mass Transfer, Vol. 17, Feb. 1974, pp. 205-214.

[17]Burde, S.S., "Thermal Contact Resistance Between Smooth Spheres and Rough Flats," Univ. of Waterloo, Ph.D. Thesis, May 1977.

[18]Yovanovich, M.M., "Thermal Constriction Resistance of Contacts on a Half-Space: Integral Formulation," AIAA Paper 75-708; also published in Progress in Astronautics and Aeronautics: Radiative Transfer and Thermal Control, Vol. 49, ed. by A.M. Smith, AIAA, N.Y., 1976, pp. 397-418.

[19]Yovanovich, M.M., Burde, S.S., and Thompson, J.C., "Thermal Constriction Resistance of Arbitrary Planar Contacts with Constant Flux," AIAA Paper 76-440, also published in Progress in Astronautics and Aeronautics: Thermophysics of Spacecraft and Outer Planet Entry Control, Vol. 56, ed. by A.M. Smith, AIAA, N.Y., 1977, pp. 127-140.